Ground-Based Bistatic Radar for Space Surveillance using a Non-Cooperative Radar Illuminator

Richard Ferranti
SRI International

ABSTRACT

A bistatic radar can be defined as a radio-based ranging system with transmitting and receiving antennas that are separated by distances on the order of the range to the target [1]. Bistatic space surveillance radar systems can provide multiple, simultaneous, independent looks at space debris, thereby enhancing detection performance. This paper proposes a method for existing high-power surveillance radars to serve as illuminating signal sources for a bistatic radar receiver without pre-knowledge of their beam-pointing angle or waveform. This information can be derived by deploying a small antenna and receiver within the line of sight of the illuminating radar. Just as a unique set of complex weights can be applied to the illuminator's phased array to scan a beam in a specific direction, so also the reference receiver can obtain complex radio frequency (RF) samples unique to those scanned antenna angles. The reference receiver thus supplies the bistatic receiver with the beam-pointing angle of its illumination as well as the transmitted waveform for its matched filter. The bistatic radar receiving system can be built with a phased-array antenna and software-defined radios (SDRs) that continuously digitize and store signals received at each element. When the illuminating radar's beam-pointing angle is determined, the receiver can beamform its stored data to form a common surveillance volume with the transmitted signal, achieving bistatic operation in near real time. The system may incorporate a machine-learning (ML) algorithm so that, for each target detection, the bistatic radar reinforces the relationship between a reference receiver's measurements and the actual illuminator's beam-pointing angle. This feature can mitigate reference measurement errors due to multipath or other propagation impediments between the illuminating radar and the reference receiver.

1. INTRODUCTION

The existing network of U.S. ground-based space, aircraft, and weather radars can be used as non-cooperative illuminators to detect space objects and debris. Ground-based receivers using multi-beam array antennas can receive bistatic reflections from space objects whenever a non-cooperating radar beam points at the space vehicle or debris. Space-object radar cross section (RCS) can be enhanced where the bistatic angle is large, providing increased detection probability for small space debris. A network of passive sensors with common beam volumes can harvest and combine multiple bistatic reflections (energy otherwise lost in space) and enhance small-object detection and target disambiguation. The goal of this research is to provide a means of achieving ground-based, bistatic space radar surveillance with passive receive-only array antennas using existing, non-cooperating radars as illuminators. While the method will work with a non-cooperating radar that uses any type of antenna, we illustrate its application to current and next-generation radar systems that use phased-array antenna technology.

Bistatic radar operation using a non-cooperative illuminator brings a number of advantages for space surveillance systems, including:

- Increased target detection capability, with the bistatic receiver(s) harvesting radar energy reflected from objects at angles other than that retroreflected to the monostatic radar.
- Decreased radar surveillance system construction costs compared with the cost of deploying multiple monostatic radars, since a passive bistatic radar antenna/receiver requires no transmitting or waste-heat-management equipment.
- Greatly decreased radar surveillance system operating costs, with no continuing multi-hundred kilowatt or megawatt-level transmitter energy expenses at bistatic receiver sites.
- Improved receiver system sensitivity, with no losses incurred by transmit-receive switching circuitry.

2. APPROACH

2.1 Overview

The three basic requirements for implementing a bistatic radar receiver are to (1) determine the timing of the transmitted pulse, so that the bistatic receiver can obtain the range to the target; (2) obtain a record of the transmitted pulse waveform and frequency, so that the receiver can build its waveform replica for matched filtering and detection; (3) determine where the transmitting station is pointing its antenna, so that the receiver can point its antenna to form a common volume containing the receiver beam, transmitter beam, and target. For a bistatic radar system with cooperating transmitter and receiver stations, all three requirements are easily fulfilled, but this is not the case when the transmitting radar is acting independently as a non-cooperative illuminator.

The proposed approach is to provide all three bistatic radar requirements for a non-cooperating illuminator by deploying a small reference antenna and receiver within line-of-sight distance to the transmitting radar.[1] The reference antenna receives sidelobe transmissions from the non-cooperating radar and records the transmitted waveform as well as its time of arrival. A wideband SDR digitizes the entire RF spectrum occupied by the non-cooperating radar and also records the transmitted waveform center frequency. These data fulfill the first two requirements (timing and waveform) by employing a matched filter that recovers the amplitude and phase of each transmitted radar pulse. As discussed below, these complex samples will also reveal the beam-pointing direction of the radar.

A phased-array radar antenna is designed to form a beam by setting the phase and amplitude of each of its array elements to values unique to that particular beam direction. It follows that if we sense the amplitude and phase of any of the antenna's sidelobes, we should be able to identify where the main beam is pointing, because those sidelobes are also determined by the particular set of complex antenna weights that steered the main beam. This method requires an accurate model of the non-cooperative radar antenna and, if our knowledge is incomplete or corrupted by other factors to be described later, will also benefit from ML augmentation.

We employed an electromagnetic (EM) simulator[2] for an initial confirmation that a broad-beam, simple reference receiver antenna can indeed provide an illuminating radar's complex samples with sufficient fidelity to identify the array's beam-pointing angle. The illuminating radar's array antenna model comprises a uniformly excited 192-element phased array (8 by 24 elements) with a simple dipole reference antenna placed in its far field. The array was steered to many beam positions by applying the appropriate phase ramps to its elements. The left side of Fig.1 shows the array's main beam and sidelobes and the position of a dipole reference antenna 500 wavelengths distant in the far field of this small phased array.

The right side of Fig. 1 shows polar plots of the amplitudes and phases of the currents induced in the dipole reference antenna as the array's main beam is steered to a number of different pointing angles. Note that for each steered beam angle shown on the plots, there is a unique complex point. Particularly interesting is the spiral-like pattern of the reference antenna samples in the lower polar plot as the array performs a coarse azimuth scan comprising four beam positions between 110 and 140 degrees elevation with the azimuth fixed at 5 degrees. This complex sample trajectory suggests that not only are individual beam-pointing directions identified by a particular complex reference sample, but also that coordinated scans (at the horizon, for example) reveal themselves by tracing unique trajectories in the complex plane. In the following section we will further investigate these patterns by using a classic mathematical model of a phased-array antenna.

---

[1] This reference antenna should be situated in the sidelobes of the non-cooperating radar antenna so that its main beam does not overload the reference receiver. Even if the non-cooperating radar's antenna sidelobes are 40 dB down from the beam peak, the radar's high transmit power will provide a very large signal-to-noise ratio at the reference antenna/receiver located at a typical line-of-sight distance of 5 or 10 km.

[2] The Numerical Electromagnetics Code, originally produced by Lawrence Livermore Laboratory and publicly available. The instantiation employed here is 4nec2, an adaptation for Windows by Arie Voors.

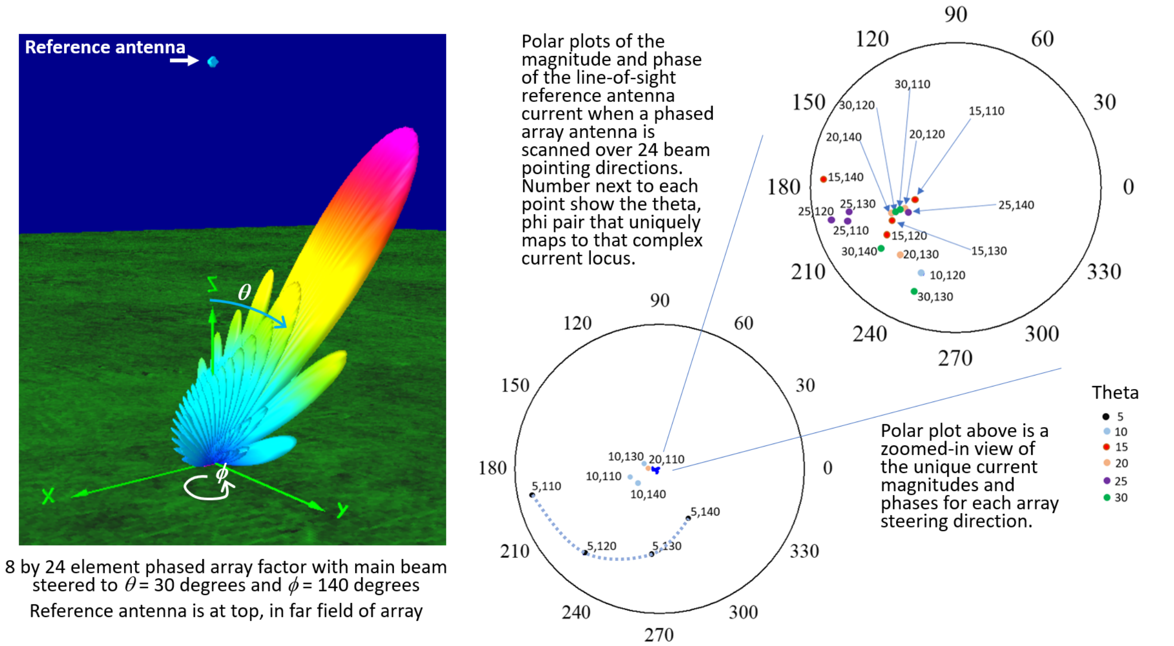

Fig. 1. Left: Array factor of an 8-by 24-element phased array antenna with far-field reference antenna at top. Right: Polar plots of the complex current induced in the reference antenna for different steering angles of the array antenna.

2.2 Phased-Array Antenna Model

In array antenna theory, the array's radiation pattern is the product of its element pattern and its array factor (AF). For this analysis we assume that each array element is an isotropic radiator, so that the array factor forms the far-field antenna pattern. As shown in [2], a rectangular array of M by N identical elements has a complex AF given by

$$AF(\theta,\phi,\theta_0,\phi_0) = I_0 \sum_{m=1}^{M} I_m \left(e^{j(m-1)(kd_x \sin\theta\cos\phi+\beta_x)}\right) \sum_{n=1}^{N} I_n \left(e^{j(n-1)(kd_y \sin\theta\sin\phi+\beta_y)}\right)$$

$$\beta_x = -kd_x \sin\theta_0 \cos\phi_0$$

$$\beta_y = -kd_y \sin\theta_0 \sin\phi_0$$

where k is the wavenumber ($2\pi/\lambda$), d_x and d_y are the spacings between x and y-directed elements in wavelengths (here 0.48λ), I_0 is an overall current scaling factor, and I_m and I_n are the weighted currents for the x and y dimensions. θ_0 and ϕ_0 define the main beam-steering direction in elevation and azimuth. This equation assumes that the weighting functions determining the currents in each element are proportional in both x and y directions.

Fig. 2 shows several conceptual components of the bistatic receiver reference system: the illuminating radar's antenna elements, array configuration, and propagation path to the bistatic reference receiver. The complex signal sample received at the reference antenna is modified by the propagation path between the radar's illuminating array and the reference antenna, which may include multipath. Over short, stable, line-of-sight distances, this path simply multiplies the AF by fixed amplitude and phase factors. Finally, the reference antenna itself will change the amplitude and phase of the signal delivered to the reference receiver. All of these factors are fixed except for the array factor of the steered illuminating radar's antenna. Thus, within a fixed scaling factor, the complex received reference signal is a sole function of the illuminating radar's array factor. The above array factor equation can then be used to rapidly model an array antenna scanned over many angles, producing continuous complex samples of the reference receiver signal multiplied by a fixed scale factor. This approach is much faster than running a full electromagnetic simulation for each beam position.

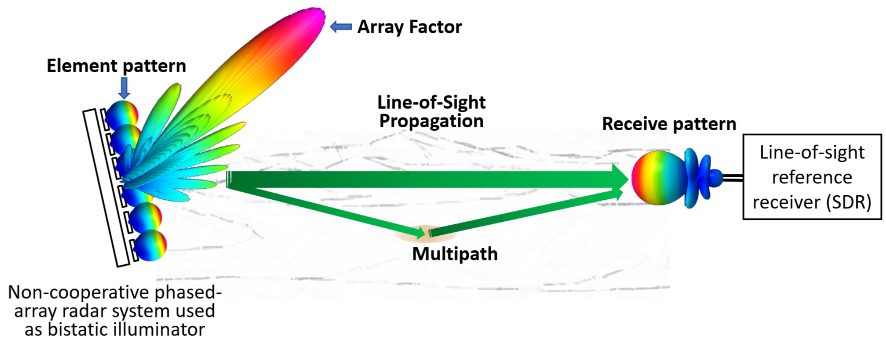

Fig. 2. The bistatic reference receiver system components, including the element and array factors of the illuminator antenna, the propagation paths, and the reference receiver antenna pattern.

The left side of Fig. 3 shows another example of an antenna's array factor from a 21 x 21 array with 441 elements and cosine weighting. It also shows the fixed reference antenna's coordinates in azimuth and elevation. The illuminating radar array factor is scanned in azimuth at four elevation angles, as shown by the lines superimposed on the 3D pattern. The resulting four complex sample traces, as sensed at the reference antenna's coordinates, are plotted in rectangular form on the two plots in the center of the figure, with each trace a different color. The same patterns are shown on the right of the figure but plotted in polar coordinates; note that this polar plot has a log magnitude radius scale.

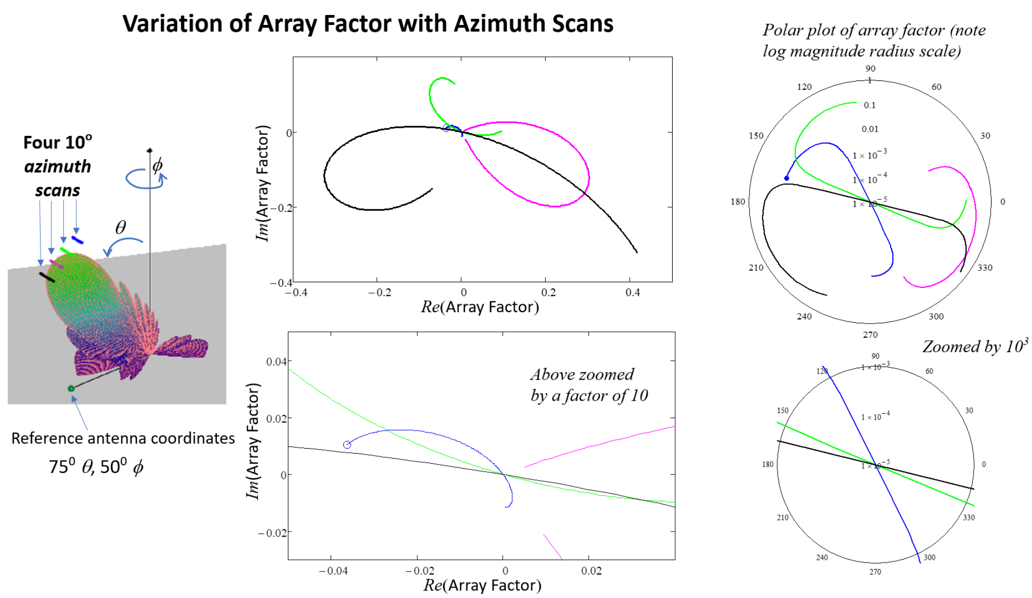

Fig. 3. Complex reference receiver samples (center and right columns) from four azimuth scans from a 441-element phased-array antenna array factor (example shown on left). Each color-coded azimuth scan is sensed at the reference antenna coordinates and plotted as trajectories in rectangular and polar coordinates.

As the antenna is scanned, the changing antenna factor presents as a different smooth trajectory for each set of scan angles. Also evident is that the complex antenna factor traces can cross each other, so that while the trajectories are unique to a particular scan, there are instances where an individual complex sample is not unique to a particular antenna-pointing direction. The lower center panel, which is a magnified version of the upper panel, also shows that multiple array factors can cross through zero (when, for example, an array factor null is precisely located at the reference antenna coordinates). Both of these ambiguities can be ameliorated: actual phased array antennas are steered with quantized phase shifters that will likely result in discrete antenna factor loci that are not coincident with each other; physically realized array antennas have finite tolerances that disallow array factor nulls that are exactly zero; and an ML algorithm (discussed later) can recognize that a scan pattern is a smoothly varying curve and does not have discontinuous derivatives.

Fig. 4 shows the same type of array factor plot but for four elevation scans, as illustrated on the antenna pattern on the left. The reference antenna coordinates are the same as in the previous figure. Again, the array factor trajectories are unique for each scan.

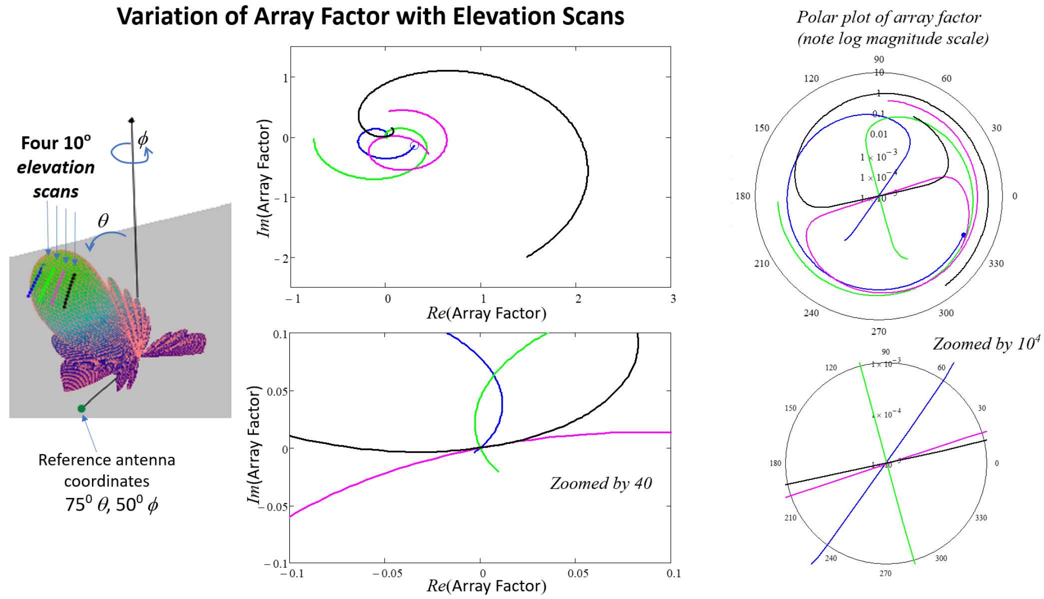

Fig. 4. Complex reference receiver sample trajectories from four elevation scans with the same array as in Fig. 3.

In Fig. 5 we illustrate an alternate case where the array factors of four slant scans are plotted, but with slightly different reference antenna coordinates. This might be the case when the reference antenna has been moved to a slightly different location. The rectangular plots in the center column appear similar but are not exactly alike. However, the polar plots on the right-hand column clearly show the phase shift (a pattern rotation) that is obtained with this slight change in reference antenna coordinates.

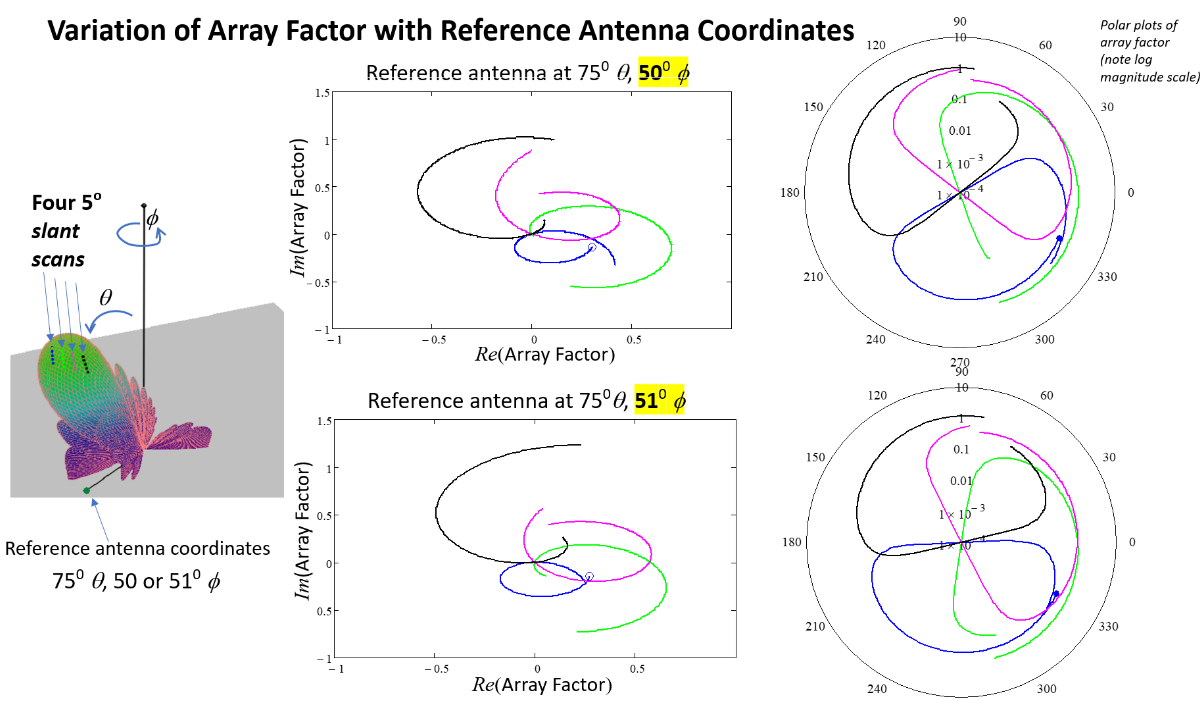

Fig. 5. The same array configuration as in Fig. 4 but showing four slant scan trajectories and the effects of a slight shift in reference antenna coordinates.

2.3 System Configuration

Fig. 6 is a block diagram suggesting how a bistatic radar receiving system with a non-cooperative radar illuminator may be configured. The reference antenna and wideband SDR receiver are located within line of sight of the non-cooperative radar illuminator, providing timing and complex waveform samples to a reference signal processor. This processor uses previously sampled and stored waveform replicas to match-filter the illuminator's pulses, forming a complex signal sample for each detected pulse. Using a model of the illuminator's antenna and the complex signal samples, the reference signal processor provides a beam angle estimate to an ML pointing angle algorithm, discussed below. The bistatic receiver array is steered so that its beam intersects the common volume containing the transmit beam and potential target.

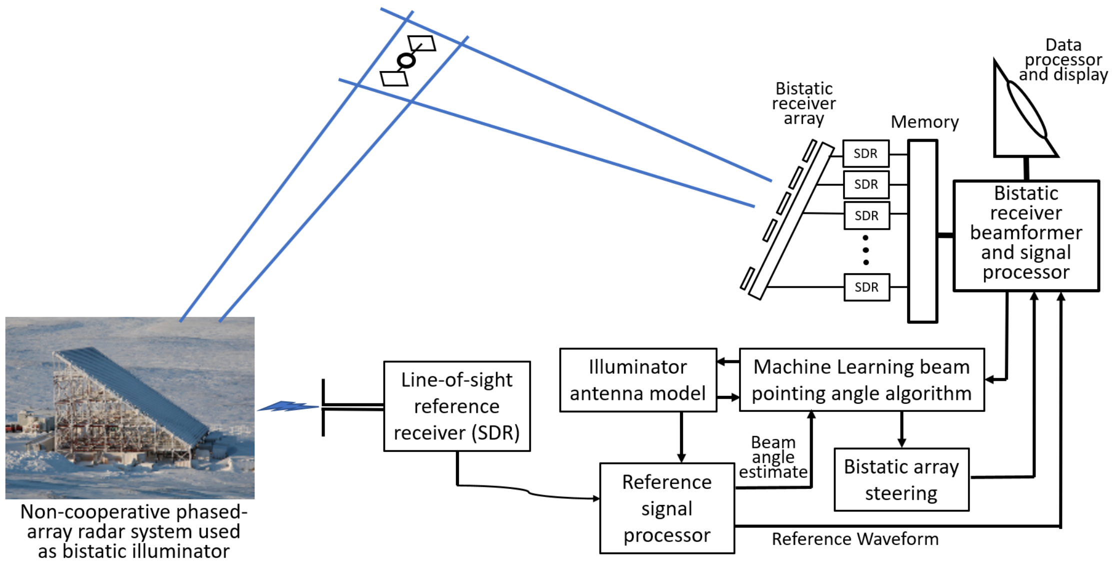

Fig. 6. Block diagram of a bistatic radar receiver system using a non-cooperative radar illuminator, incorporating a reference antenna and receiver located within line of sight of the transmitter antenna .

The bistatic receiver array could have a single SDR and beamformer, or as shown in the figure, as many as one SDR per antenna element, giving it the ability to form multiple simultaneous receive beams. For the latter case, the SDR outputs could be stored in a temporary memory so that the multiple beams can be examined for target detections in near real time, with each beam steered to likely bistatic locations provided by the ML pointing algorithm. A target detection would provide confirmation to the ML that the reference sample was correctly associated with a likely beam pointing angle, and the antenna model appropriately updated. The rest of the system comprises standard radar processing techniques such as target metrics extraction, tracking, and display.

Note that a memory placed between the bistatic receiver array and its signal processor also allows for the processing and transmission time of the reference receiver data to the rest of the system, which could be hundreds of kilometers distant.

2.4 Machine learning considerations

Machine learning augmentation is an important aid in determining scan patterns and disambiguating individual beam-pointing directions from the complex samples provided by the reference receiver. As in all such techniques, ML will require a great deal of modeled and observational data to train the system. This training is used to recognize samples and patterns that it has previously encountered, and to accurately identify a known beam-pointing angle. To successfully interpolate to unseen or rarely seen pointing positions, it is important to note that the illuminating radars usually operate continuously, providing tens or hundreds of thousands of reference receiver samples per day, each a learning opportunity for the algorithm. Every successful target detection, which indicates a match between reference receiver sample and the correct bistatic radar beam pointing angle, reinforces the ML process. This holds for scan pattern trajectories as well. And as mentioned above, phased-array radars utilize quantized phase shifters, so these illuminators have a finite number of possible beam positions. Thus, the ML algorithm does not have to consider an infinite variation in possible complex sample values and their associated beam angles.

Machine learning can also provide benefit for instances where the propagation path between the illuminating radar and reference receiver changes. These changes should be minimized by proper siting of the reference antenna (high, in the clear, and with direct line of sight with the illuminating radar), but occasional signal impediments like unstable multipath or severe rain fading can be modeled as part of the ML training set.

2.5 Failed elements modeling

One of the features of a radar employing a phased-array antenna comprising hundreds or thousands of elements is that failed elements do not cause total system failure; that is, the radar system is said to degrade "gracefully." The downside of this feature is that handfuls of dead elements are usually tolerated, so that the radar is never operating at its peak performance. Since the non-cooperative bistatic radar method outlined above depends on accurate knowledge of the illuminator's antenna array factor, how will random failed antenna elements affect this critical parameter?

To explore failed element effects, we return to the electromagnetic simulation of the 192-element rectangular phased array (8 x 24 elements), this time with uniform illumination in the 8-element direction but Taylor weighting (35 dB sidelobes, nbar = 5) in the 24-element direction. As above, a simple dipole reference antenna is placed in its far field. For the first three trials, we randomly placed 9 failed elements (i.e., the element positions have their antennas still present but with no excitation, simulating a failed transmitter) and plotted the complex response at the reference antenna. The physical antenna faces with their failed element locations are shown in the left column of Fig. 7, with the antenna factor for a perfect antenna and one with failed elements also shown. As expected, the sidelobe levels grow for the failed element cases, without much difference in the main lobe. The right column in the figure shows the complex responses of the reference antenna in rectangular and polar coordinates for the three cases. The complex sample loci move, though they appear to follow a linear trajectory in the polar plot.

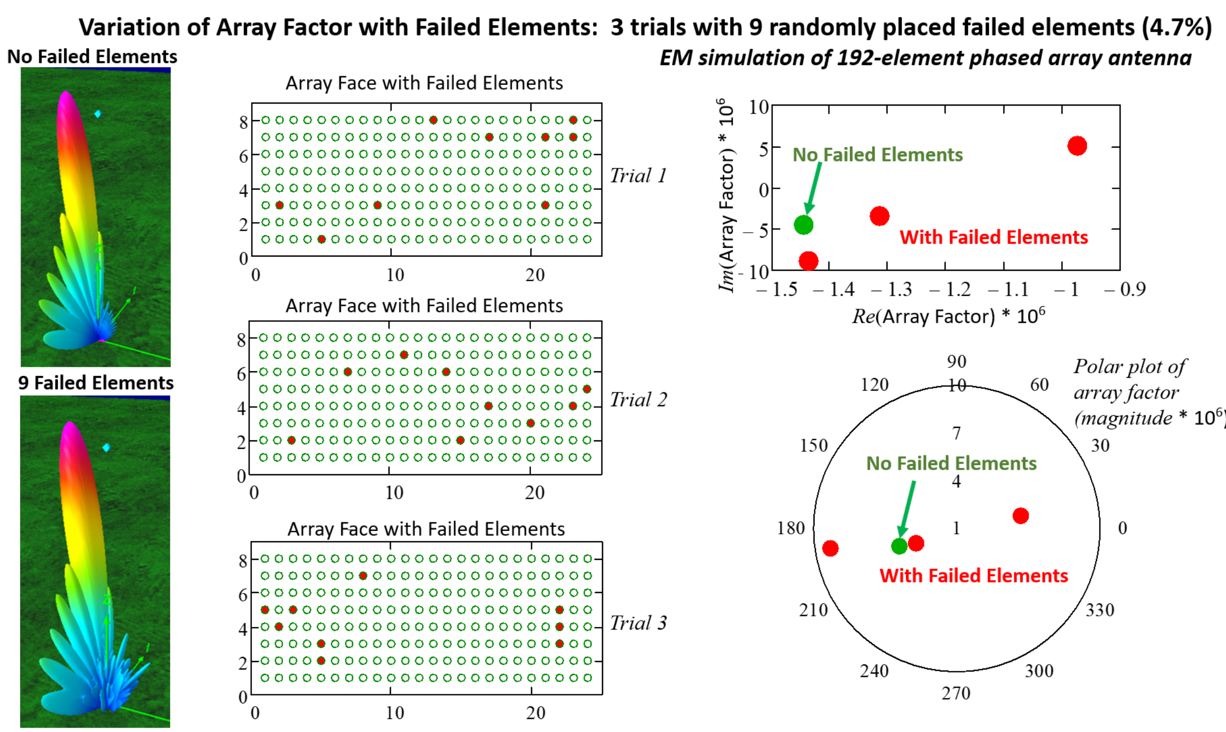

Fig. 7. EM simulations for a 192-element array with three trials of 9 failed elements. Left side shows array factors with no and 9 failed elements and their locations on the array face. Right column shows the complex array factor samples in rectangular and polar form.

In Fig. 8, we show a more dramatic example with 35 randomly placed failed elements (18.2% of the total), again over three trials. The AF sidelobes grow higher than the 9 failed element case, and again, the reference antenna's complex samples exhibit a linear behavior on the polar plot. A deeper understanding this intriguing linear behavior would take many more simulations of randomly failed elements on larger arrays, but from these examples it appears that an ML-based correction for failed elements may benefit from the linear correlation.

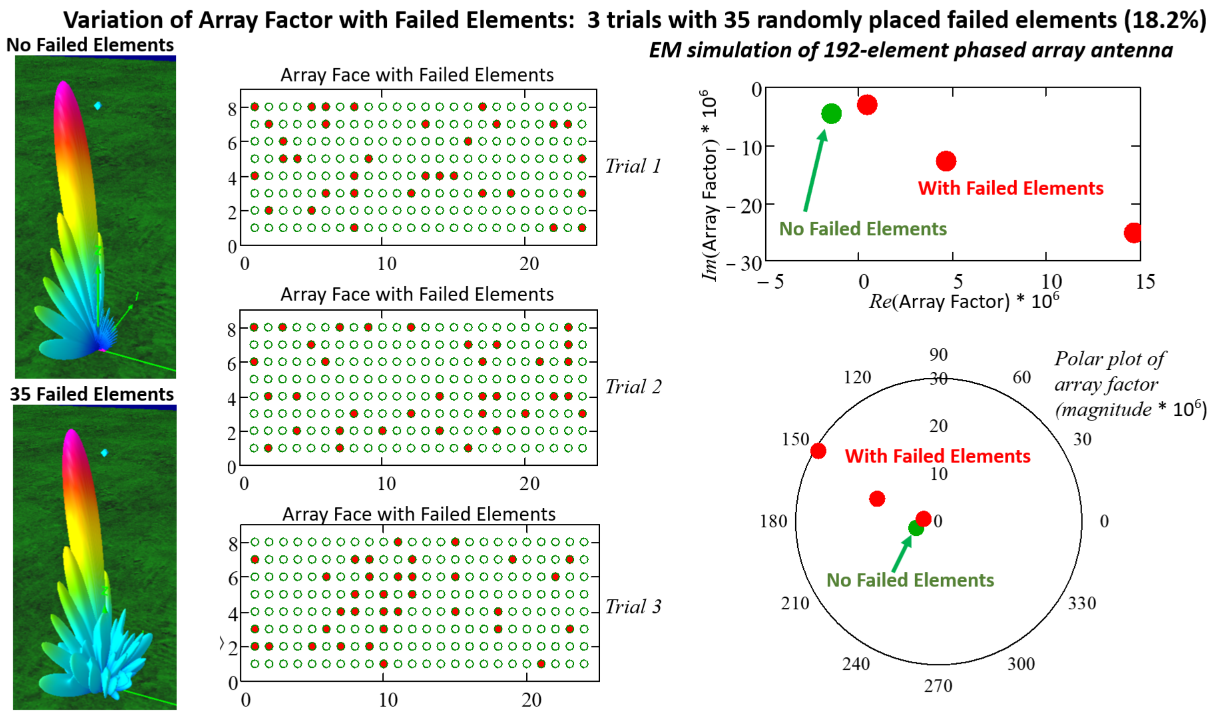

Fig. 8. Same as Fig. 7, with three trials of 35 failed elements in the 192-element array. Note the higher array factor sidelobe levels and the same linear relationship among trials as the 9-failed-element simulation.

3. CONCLUSIONS

Bistatic radars offer increased detection performance because they harvest energy reflected by targets at angles other than the retroreflected signal received by a monostatic system. A bistatic radar receiver does not require expensive transmitting equipment, nor do its operating costs include large transmitter power expenditures. This paper presents a method for achieving bistatic operation with a non-cooperating phased-array radar by deploying nearby a reference antenna and receiver. The receiver supplies the timing, reference waveform, and especially the non-cooperative radar's beam-pointing direction. It achieves the latter by employing a model of the non-cooperating radar's antenna and measuring a complex sample of the transmitted pulse, which is highly correlated with the antenna beam position. When the non-cooperating illuminator's antenna is scanned over a particular track, the locus of received complex samples traces a unique trajectory. We provide a high-level, non-cooperative bistatic radar receiver system diagram, investigate anomalies caused by propagation and non-cooperating radar phased-array element failures, and consider ML augmentation to address these conditions.

4. REFERENCES

[1] N. J. Willis, *Bistatic Radar*, Artech House, 1991, Section 1.2.
[2] C.A. Balanis, *Antenna Theory Analysis and Design*, Harper and Row, 1982, p. 261.